Hu, E., Liang, P. & Spiegelman, B.M. (1996) AdipoQ is a novel adipose-specific gene dysregulated in obesity. *Journal of Biological Chemistry*, **271**, 10697–10703.

Kern, P.A., Di Gregorio, G.B., Lu, T., Rassouli, N. & Ranganathan, G. (2003) Adiponectin expression from human adipose tissue: relation to obesity, insulin resistance, and tomour necrosis factor-alpha expression. *Diabetese*, **52**, 1779–1785.

Krogh-Madsen, R., Plomgaard, P., Keller, P., Keller, C. & Pedersen, B.K. (2003) Insulin stimulates interleukin-6 and tumour necrosis factor-alpha gene expression in human subcutaneous adipose tissue. *Am J Physiol Endocrinol Metabolism*, **286**, E234–E238.

Lindsay, R.S., Walker, J.D., Havel, P.J., Hamilton, B.A., Calder, A.A., Johnstone, F.D. & Scottish Multicentre Study of Diabetes Pregnancy. (2003) Adiponectin is present in cord blood but is unrelated to birth weight. *Diabetes Care*, **26**, 2244–2249.

Maeda, K., Okubo, K., Shimomura, I., Funahashi, T., Matsuzawa, Y. & Matsubara, K. (1996) cDNA cloning and expression of a novel adipose specific collagen-like factor, apM1 (AdiPose Most abundant Gene transcript 1). *Biochemical and Biophysical Research Communications*, **221**, 286–289.

Matsubara, M., Katayose, S. & Maruoka, S. (2003) Decreased plasma adiponectin concentrations in nondiabetic women with elevated homeostasis model assessment ratios. *European Journal of Endocrinology*, **148**, 343–350.

Matsuda, J., Yokota, I., Iida, M., Murakami, T., Naito, E., Ito, M., Shima, K. & Kuroda, Y. (1997) Serum leptin concentration in cord blood: Relationship to birth weight and gender. *Journal of Clinical Endocrinology and Metabolism*, **82**, 1642–1644.

Matsuda, J., Yokota, I., Iida, M., Murakami, T., Yamada, M., Saijo, T., Naito, E., Ito, M., Shima, K. & Kuroda, Y. (1999) Dynamic changes in serum leptin concentrations during the fetal and neonatal periods. *Pediatric Research*, **45**, 71–75.

Motoshima, H., Wu, X., Sinha, M.K., Hardy, V.E., Rosato, E.L., Barbot, D.J., Rosato, F.E. & Goldstein, B.J. (2002) Differential regulation of adiponectin secretion from cultured human omental and subcutaneous adipocytes: effects of insulin and rosiglitazone. *Journal of Clinical Endocrinology and Metabolism*, **87**, 5662–5667.

Nakano, Y., Tobe, T., Choi-Miura, N.H., Mazda, T. & Tomita, M. (1996) Isolation and characterization of GBP28, a novel gelatin-binding protein purified from human plasma. *Journal of Biochemistry*, **120**, 803–812.

Nishizawa, H., Shimomura, I., Kishida, K., Maeda, N., Kuriyama, H., Nagaretani, H., Matsuda, M., Kondo, H., Furuyama, N., Kihara, S., Nakamura, T., Tochino, Y., Funahash, T. & Matsuzawa. Y. (2002) Androgens decrease plasma adiponectin, an insulin-sensitizing adipocyte-derived protein. *Diabetes*, **51**, 2734–2741.

Ong, K., Kratzsch, J., Kiess, W., Costello, M., Scott, C. & Dunger, D. (2000) Size at birth and cord blood levels of insulin, insulin-like growth factor I (IGF-I), IGF-II, IGF-binding protein-1 (IGFBP-1), IGFBP-3, and the soluble IGF-II/mannose-6-phosphate receptor in term human infants. The ALSPAC Study Team. Avon Longitudinal Study of Pregnancy and Childhood. *Journal of Clinical Endocrinology and Metabolism*, **85**, 4266–4269.

Picaud, J.C., Rigo, J., Nyamugabo, K., Milet, J. & Senterre, J. (1996) Evaluation of dual-energy X-ray absorptiometry for body-composition assessment in piglets and term human neonates. *American Journal of Clinical Nutrition*, **63**, 157–163.

Scherer, P.E., Williams, S., Fogliano, M., Baldini, G. & Lodish, H.F. (1995) A novel serum protein similar to C1q, produced exclusively in adipocytes. *Journal of Biological Chemistry*, **270**, 26746–26749.

Schubring, C., Kiess, W., Englaro, P., Rascher, W., Dotsch, J., Hanitsch, S., Attanasio, A. & Blum, W.F. (1997) Levels of leptin in maternal serum, amniotic fluid, and arterial and venous cord blood: relation to neonatal and placental weight. *Journal of Clinical Endocrinology and Metabolism*, **82**, 1480–1483.

Soriguer Escofet, F.J., Esteva de Antonio, I., Tinahones, F.J. & Pareja, A. (1996) Adipose tissue fatty acids and size and number of fat cells from birth to 9 years of age – a cross-sectional study in 96 boys. *Metabolism*, **45**, 1395–1401.

Soto, N., Bazaes, R.A., Pena, V., Salazar, T., Avila, A., Iniguez, G., Ong, K.K., Dunger, D.B. & Mericq, M.V. (2003) Insulin sensitivity and secretion are related to catch-up growth in small-for-gestational-age infants at age 1 year: results from a prospective cohort. *Journal of Clinical Endocrinology and Metabolism*, **88**, 3645–3650.

Stefan, N., Bunt, J.C., Salbe, A.D., Funahashi, T., Matsuzawa, Y. & Tataranni, P.A. (2002) Plasma adiponectin concentrations in children: relationships with obesity and insulinemia. *Journal of Clinical Endocrinology and Metabolism*, **87**, 4652–4656.

White, D.R., Widdowson, E.M., Woodard, H.Q. & Dickerson, J.W. (1991) The composition of body tissues (II). Fetus to young adult. *British Journal of Radiology*, **64**, 149–159.

Wolfe, H.M., Brans, Y.W., Gross, T.L., Bhatia, R.K. & Sokol, R.J. (1990) Correlation of commonly used measures of intrauterine growth with estimated neonatal body fat. *Biology Neonate*, **57**, 167–171.

Yamauchi, T., Kamon, J., Minokoshi, Y., Ito, Y., Waki, H., Uchida, S., Yamashita, S., Noda, M., Kita, S., Ueki, K., Eto, K., Akanuma, Y., Froguel, P., Foufelle, F., Ferre, P., Carling, D., Kimura, S., Nagai, R., Kahn, B.B. & Kadowaki, T. (2002) Adiponectin stimulates glucose utilization and fatty-acid oxidation by activating AMP-activated protein kinase. *Nature Medicine*, **8**, 1288–1295.

Zhang, Y., Proenca, R., Maffei, M., Barone, M., Leopold, L. & Friedman, J.M. (1994) Positional cloning of the mouse obese gene and its human homologue. *Nature*, **372**, 425–432.

脳と発達 2004：36；324－329

＝症例報告＝

臨床的Leigh脳症を呈したメチルマロン酸血症の1例

伊藤 弘道[1] 森 健治[1] 伊藤 道徳[1,2]
内藤 悦雄[1] 横田 一郎[1] 黒田 泰弘[1]

要旨 臨床的にLeigh脳症と考えられる左右対称性の大脳基底核病変を認め，vitamin B_1投与により画像所見，臨床症状の著明な改善が認められたメチルマロン酸血症の1例を経験した．本症例においてvitamin B_1が著効したことから，メチルマロニルCoA蓄積によるピルビン酸カルボキシラーゼ活性の阻害に加えて急性増悪時の治療におけるvitamin B_1欠乏によるエネルギー産生障害，特にピルビン酸脱水素酵素複合体活性の阻害が生じたことが臨床的Leigh脳症の原因と考えられる．このことから，メチルマロン酸血症の治療においては，vitamin B_1の欠乏に対して十分に注意し，急性増悪時の輸液療法では，vitamin B_1を加えることが必要であると考えられた．

見出し語 メチルマロン酸血症，Leigh脳症，vitamin B_1，大脳基底核，^{1}H-magnetic resonance spectroscopy (^{1}H-MRS)

はじめに

Leigh脳症は，視床，大脳基底核，中脳，橋などの左右対称性の壊死性病変（脳病理組織学的には神経細胞の脱落，グリア細胞の増加，毛細血管の増生等）を特徴とし退行性神経症状を呈する疾患で，神経病理学的診断名であるため，剖検所見により確定診断されるが，最近の画像診断法の進歩により，頭部CTやMRIなどにより臨床的にLeigh脳症と診断されるようになってきている．その基礎疾患としては，ピルビン酸代謝異常症，ミトコンドリア電子伝達系異常症，有機酸代謝異常症などが報告されている．しかしながら，これまでに臨床的Leigh脳症をきたしたメチルマロン酸血症の報告は我々が調べえた範囲においては認められなかった．今回我々は，メチルマロニルCoA蓄積によるピルビン酸代謝障害に加えて，急性増悪時の治療におけるvitamin B_1欠乏がその原因と考えられる臨床的Leigh脳症を伴ったメチルマロン酸血症の1例を経験したので報告する．

[1]徳島大学医学部発生発達医学講座小児医学分野
[2]国立病院機構香川小児病院小児科

連絡先 〒770-8503 徳島市蔵本町3-18-15
徳島大学医学部発生発達医学講座小児医学分野
(伊藤弘道)

(受付日：2003. 7. 2，受理日：2003. 11. 6)

I 症 例

患 者 1歳1カ月，男児．

主 訴 食欲低下，嘔吐，意識障害．

家族歴 近親婚なし．家系内に新生児期に死亡した者はいない．

現病歴 在胎39週5日，3,000 g，正常分娩にて出生．仮死は認めなかった．頸定は3カ月．その後，筋緊張低下，精神運動発達遅延を認め，近医にて経過観察されていた．11カ月時にはお座りは可能となったが，12カ月時でも寝返り，四つ這いは不可，模倣，有意語も認めず，津守・稲毛式によるDQは56であった．また，生後5カ月頃より咳，鼻汁，喘鳴を繰り返し訴え，近医をよく受診していた．生後11カ月からはその症状が徐々に増強し，12カ

表1 検査成績

検血		CK	7 IU/l
WBC	11.0 × 10³/μl	BS	82 mg/dl
RBC	445 × 10⁴/μl	NH_3	83 μg/dl
Hb	12.4 g/dl	乳酸	21.3 mg/dl
Ht	37.1%	ピルビン酸	1.6 mg/dl
Plt	40.5 × 10⁴/μl	総カルニチン	21.8 μmol/l
免疫血清		遊離カルニチン	11.5 μmol/l
CRP	< 0.01 mg/dl	アシルカルニチン	10.3 μmol/l
生化学		血液ガス毛細管血	
TP	6.9 g/dl	pH	7.358
GOT	24 IU/l	HCO_3	12 mmol/l
GPT	14 IU/l	BE	− 13 mmol/l
LDH	506 IU/l	PCO_2	22.1 mmHg
ALP	272 IU/l	髄液	
T-Bil	0.7 mg/dl	細胞数	2/3
BUN	16 mg/dl	蛋白	15 mg/dl
Cre	0.2 mg/dl	糖	63 mg/dl
Na	135 mEq/l	乳酸	22.1 mg/dl
K	3.5 mEq/l	ピルビン酸	1.8 mg/dl
Cl	104 mEq/l		

月時には上記症状に加えて食欲が極端に低下し，頻回の嘔吐も認められるようになったため，喘息様気管支炎の診断で近医に入院し，vitaminを含まない輸液療法が開始された．入院後も食欲低下，頻回の嘔吐は改善されず，入院10日目には傾眠状態となったため，翌日精査加療目的で当科に紹介され，入院となった．

入院時現症 身長76.1 cm，体重9,780 g，頭囲48.0 cm，脈拍数108/min，呼吸数36/min，意識レベルはJapan Coma Scaleで30であった．眼球運動では眼振，共同偏視等の異常は認めなかった．肺野では呼気性喘鳴が聴取され，腹部は平坦，軟で肝脾腫を認めなかった．また，全身で筋緊張低下を認め，自発的な四肢の運動はほとんどみられなかった．また，Scarf徴候および踵－耳試験は陽性で，引き起こし反射では頭は後方へ垂れ下がり，上肢は伸展していた．頸定は認められず，腹臥位での頭部挙上も認めなかった．深部腱反射は正常，Babinski反射は陰性で，Kernig徴候，項部硬直もみられなかった．

検査成績（表1） 検血一般検査では異常はなく，血液生化学検査では血中NH_3が83 μg/dlと軽度上昇している以外は異常所見を認めなかった．血中乳酸は21.3 mg/dl，ピルビン酸は1.6 mg/dlと軽度増加していた．血液ガス（毛細管血）分析ではpH 7.358，HCO_3 12 mmol/l，BE −013 mmol/l，pCO_2 22.1 mmHgと代謝性アシドーシスを呼吸性に代償している所見が認められた．髄液検査では，乳酸22.1 mg/dl，ピルビン酸1.8 mg/dlと軽度の増加を認め，細胞数は2/3，蛋白は15 mg/dl，糖は63 mg/dlと正常であった．尿検査ではケトン体が（＋）である以外は異常を認めなかった．血中総カルニチンは21.8 μmol/l（基準値：45.0 ～ 91.0 μmol/l），血中遊離カルニチンは11.5 μmol/l（基準値：36.0 ～ 74.0 μmol/l）とそれぞれ著明に低下していたが，血中アシルカルニチンは10.3 μmol/l（基準値：6.0 ～ 23.0 μmol/l）と正常範囲内であった．血中アミノ酸分析では，glycine，glutamic acidが増加していた．尿中アミノ酸分析では，glycineの排泄増多が，尿中有機酸分析では，methylmalonic acid，methylcitric acid，3-OH butylic acidの著明な排泄増多が認められた．脳波検査では，覚醒時基礎波の軽度徐波化，睡眠紡錘波の欠如が認められたが，発作波はみられなかった．また，聴性脳幹反応は正常であった．

入院後経過 経口摂取が不可能な状態であったにもかかわらず，近医にてvitamin B_1の含まれていない輸液療法を10日間受けていたことを考慮して，入院後ただちにvitamin B_1（12 mg/日）を含む輸液を開始したところ，翌日には全身状態および意識状態の改善が認められた．入院3日目の頭部CT検査にて両側大脳基底核に左右対称性の低吸収域を認め，

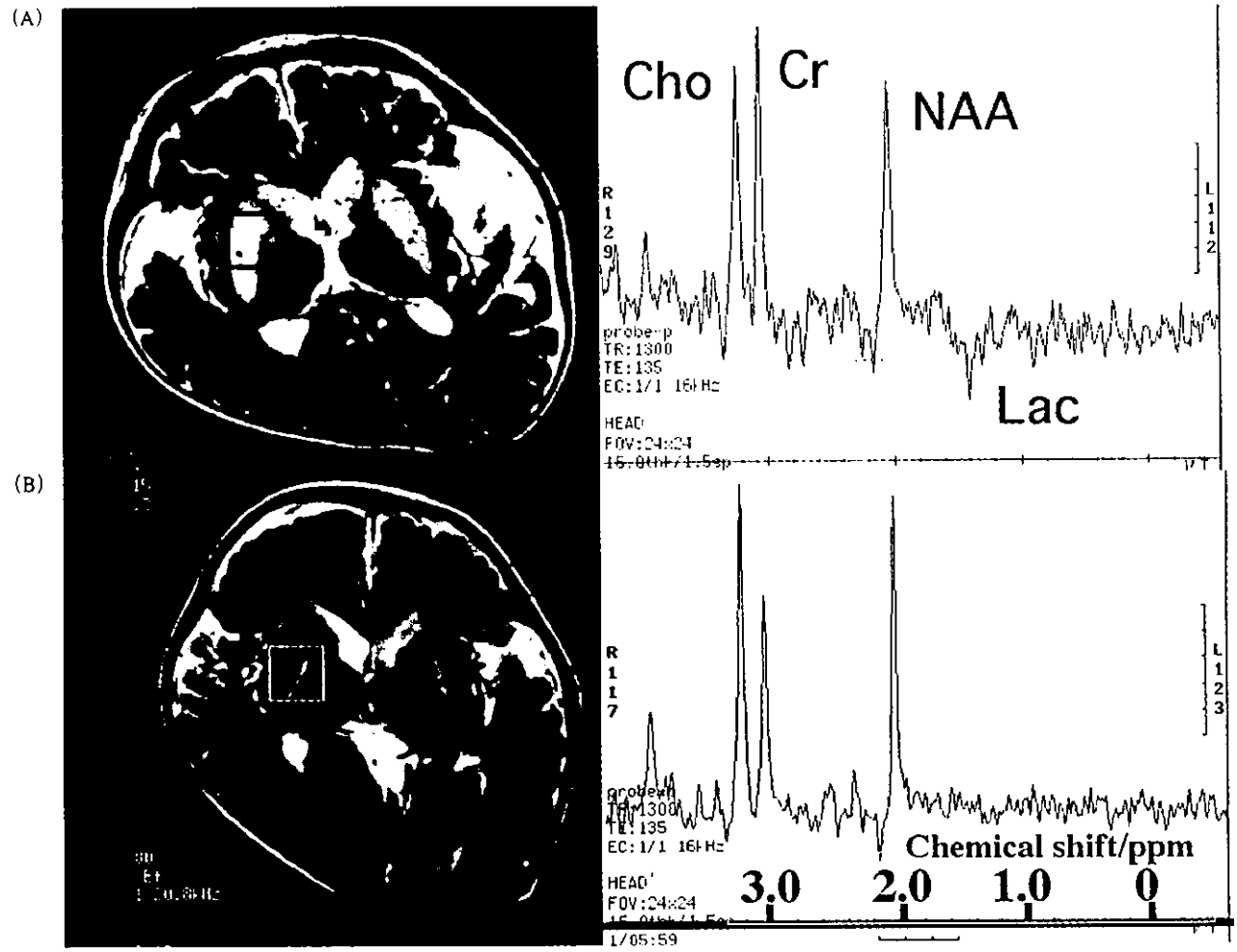

図1 頭部 MRIT$_2$ 強調画像と ^{1}H-MRS の経時的変化

A：入院時，B：入院4カ月後

入院時には頭部 MRI T_2 強調画像で，尾状核，被殻，淡蒼球に左右対称性に高信号域を認めた．^{1}H-MRS については被殻，淡蒼球において NAA/Cr 比の著明な低下と乳酸のピークを認めた．入院4カ月後の頭部 MRIT$_2$ 強調画像では左右尾状核，被殻，淡蒼球の高信号域は著明に縮小したが，萎縮を認めた．^{1}H-MRS については被殻，淡蒼球において NAA/Cr 比の上昇と乳酸のピークの消失を認めた．

入院4日目に施行した頭部 MRI 検査では，T_2 強調画像で両側大脳基底核（尾状核，被殻，淡蒼球）に左右対称性に高信号域を認めたため（図1），臨床的 Leigh 脳症と診断し，vitamin B_1（100 mg/日）と coenzyme Q（15 mg/日）の経口投与を開始した．その後，入院時に採取した尿での有機酸分析において methylmalonic acid，methylcitric acid の著明な排泄増多が認められたため，メチルマロン酸血症と診断した．次に vitamin B_{12} 反応性および不応性の鑑別のために vitamin B_{12} 負荷試験を施行したが，尿中メチルマロン酸排泄量の改善は認められず，vitamin B_{12} 不応性メチルマロン酸血症と考え，イソロイシン，バリン，スレオニン除去ミルクを用いた低蛋白食事療法を開始した．末梢血白血球を用いたメチルマロニル CoA ムターゼ活性の測定では，患児の活性は測定限界以下であり，メチルマロン酸血症と確定診断された．15カ月時には，筋緊張低下は改善し，ハイハイ，つかまり立ちはまだ不可能であったが，左右追視，お座り，寝返りは可能となり，おもちゃを見せると取りに来るようになった．また，有意語は認められないものの「アー，ウー」といった発語は可能となった．津守・稲毛式 DQ は17カ月時点で47であり，両側の尾状核，被殻，淡蒼球の障害により出現が予想された不随意運動はこの時点では出現していなかった．

入院後の頭部 MRI の経時的検討では，入院4日目に認められた T_2 強調画像での両側大脳基底核における左右対称性の高信号域は2週間後には改善を認め，

4カ月後には，尾状核，被殻，淡蒼球の萎縮は残っているもののさらに改善していた（図1）．PRESS法（TR＝1300 ms，TE＝135 ms，256回積算）による頭部^{1}H-magnetic resonance spectroscopy（^{1}H-MRS）では，関心領域として設定した被殻，淡蒼球において乳酸のピークとともにN-acetylaspartate／creatine＋phosphocreatine（NAA／Cr）比の著明な低下（0.80, 1歳正常対照1.56±0.08，－9.5SD）が認められた．4カ月後の^{1}H-MRSでは乳酸のピークは消失し，NAA/Cr比は1.37（－2.38SD）と正常対照に比して低値ではあるものの改善していた（図1）．

Ⅱ 考　　察

Leigh脳症の概念は，1951年にLeighが原因不明の退行性神経症状を呈して亜急性の経過で死亡し，特徴的な病理所見を認めた7カ月男児例を亜急性壊死性脳症として初めて報告したことに始まる[1]．Leigh脳症は本来神経病理学的診断名であるため，その確定診断には剖検所見が必要であるが，神経症状と高乳酸血症に加えて，頭部CTあるいはMRIで左右対称性の病変を大脳基底核部中心に認めた場合には，臨床的Leigh脳症と考え，原因検索を行う必要がある．また，Leigh脳症に類似した左右対称性の病変を示す疾患として，vitamin B_1欠乏によるWernicke脳症が知られており，両者の鑑別は非常に重要である．両者は画像上障害されている部位が一般に異なっている．Leigh脳症での典型的なCT，MRI所見としては，左右対称性に基底核，脳幹部を中心に病変が認められる[2)~5)]．左右対称性基底核病変は尾状核，被殻，淡蒼球すべてに及ぶが，特に被殻病変が多く報告されている．それに対して，Wernicke脳症では左右対称性に第3脳室，中脳水道，第4脳室周囲，乳頭体，視床を中心に病変が認められる[6)7)]のが一般的である．但し，これらは参考所見であり，画像所見だけで両者を完全に鑑別するのは困難と思われる．また，臨床症状としては，Leigh脳症では，食事摂取障害，精神運動発達遅延，退行，筋緊張低下，視神経萎縮，視力障害，けいれん，呼吸障害，小脳症状等が知られている[8)]．Wernicke脳症の3主徴は眼球運動障害，運動失調，精神障害であり，その中でも眼球運動障害の出現頻度は非常に高い．

本症例ではMRI画像上，Wernicke脳症よりもLeigh脳症をより強く示唆する所見が認められること，臨床症状として生後3カ月以降より筋緊張低下，精神運動発達遅延が認められ，慢性的にエネルギー代謝障害を示唆する症状を認めることより，臨床的Leigh脳症と診断した．

本症例における病因検索では，尿中有機酸分析および酵素診断によりメチルマロン酸血症と確定診断された．メチルマロン酸血症では，ケトアシドーシス発作後，錐体路障害，ジストニアや舞踏アテトーゼ等の異常姿勢，不随意運動，痙性麻痺が出現し，その際両側淡蒼球に左右対称性の，CTで低吸収域，MRI T_2強調画像にて高信号域を認めることが報告されている[9)~12)]．メチルマロン酸血症における淡蒼球障害の原因として，Heidenreichら[10)]は，一連のプロピオン酸分解過程における代謝産物の増加を，下泉ら[11)]はケトアシドーシス発作そのものを推測している．この様に一般にメチルマロン酸血症においての対称性基底核病変は淡蒼球に限局しているとされている．メチルマロン酸血症では，メチルマロニルCoA蓄積によるピルビン酸カルボキシラーゼ活性の阻害が起こり，慢性的ピルビン酸代謝障害の状態にあると考えられる．ラットの肝臓においてはメチルマロン酸の蓄積がTCAサイクルに関与するコハク酸脱水素酵素の活性を阻害することにより，エネルギー代謝障害を引き起こすとの報告もある[13)]．本症例では経口摂取不良に加えて，vitamin B_1が十分に補給されなかったことにより，vitamin B_1を補酵素とするピルビン酸脱水素酵素複合体活性も阻害され，Leigh脳症が急激に増悪し，淡蒼球のみでなく，尾状核，被殻にも障害が生じたと考えられた．したがって，メチルマロン酸血症患者では常にvitamin B_1欠乏に注意し，特に急性増悪時の輸液療法の際にはカルニチンの経口投与とともに輸液中にvitamin B_1を加えることが必要である．

内藤によると，Leigh脳症の病因としてピルビン酸代謝経路を主としたエネルギー代謝障害が考えられており[14)]，その基礎疾患としてピルビン酸脱水素酵素複合体欠損，複合体Ⅳ欠損，その他呼吸鎖の複合体欠損の一部（複合体Ⅰ，複合体Ⅱ，ATP合成酵素），ビオチニダーゼ欠損があるとしている[15)]．これまで臨床的Leigh脳症をきたしたメチルマロン酸血症の報告は我々の調べえた範囲においては認められず，今後臨床的Leigh脳症の鑑別診断の一つとして

メチルマロン酸血症も考慮する必要があると考えられる．

本症例の入院時の頭部 ^{1}H-MRS 検査における NAA/Cr 比は，0.80 と当院における 1 歳正常児の NAA/Cr 比 1.56 ± 0.08（平均± SD）に比して－9.5SD と著明に低値であり，入院後 4 カ月の時点でも 1.37（－2.38SD）と改善は認められるものの低値を示していた．NAA は神経細胞に特異的なアミノ酸と考えられており[16]，NAA のピークの低下は，神経細胞の消失やその機能低下，すなわちミトコンドリアにおける NAA 合成能の低下を反映すると考えられている[17]．本症例での症状が改善した入院 4 カ月時点での NAA/Cr 比の改善は可逆性の神経細胞の活動の低下が改善したことを反映しているものと考えられる．しかしながら，NAA/Cr 比がこの時点でも正常対照に比して低値で，尾状核，被殻，淡蒼球において萎縮が残存していることは，本症例において不可逆的な神経細胞の壊死も存在したことを反映しているものと考えられる．

尿中有機酸分析を行っていただいた，島根医科大学小児科の木村正彦先生，山口清次教授，血中メチルマロニル CoA ムターゼ活性を測定していただいた広島大学医学部小児科の佐倉伸夫先生に深謝いたします．

文　献

1) Leigh D. Subacute necrotizing encephalomyelopathy in infant. *J Neurosurg Psychiatry* 1951;**14**:216-21.
2) Koch TK, Yee MH, Hutchinson HT, Berg BO. Magnetic resonance imaging in subacute necrotizing encephalomyelopathy (Leigh's disease). *Ann Neurol* 1986;**19**:605-7.
3) Greenberg SB, Faerber EN, Riviello JJ, de Leon G, Capitanio MA. Subacute necrotizing encephalomyelopathy (Leigh disease): CT and MRI appearances. *Pediatr Radiol* 1990;**21**:5-8.
4) Geyer CA, Sartor KJ, Prensky AJ, Abramson CL, Hodges FJ, Gado MH. Leigh disease (subacute necrotizing encephalomyelopathy): CT and MR in five cases. *J Comput Assist Tomogr* 1988;**12**:40-4.
5) Medina L, Chi TL, DeVivo DC, Hilal SK. MR findings in patient with subacute necrotizing encephalomyelopathy (Leigh syndrome): correlation with biochemical defect. *Am J Roentgenol AJR* 1990;**154**:1269-74.
6) Suzuki S, Ichijo M, Fujii H, Matsuoka Y, Ogawa Y. Acute Wernicke's encephalopathy: comparison of magnetic resonance images and autopsy findings. *Intern Med* 1996;**35**:831-4.
7) Chu K, Kang DW, Kim HJ, Lee YS, Park SH. Diffusion-weighted imaging abnormalities in Wernicke encephalopathy: reversible cytotoxic edema? *Arch Neurol* 2002;**59**:123-7.
8) van Erven PM, Cillessen JP, Eekhoff EM, et al. Leigh syndrome, a mitochondrial encephalo (myo) pathy. A review of the literature. *Clin Neurol Neurosurg* 1987;**89**:217-30.
9) Korf B, Wallman JK, Levy HL. Bilateral lucency of the globus pallidus complicating methylmalonic acidemia. *Ann Neurol* 1986;**20**:364-6.
10) Heidenreich R, Natowicz M, Hainline BE, et al. Acute extrapyramidal syndrome in methylmalonic acidemia: metabolic stroke involving the globus pallidus. *J Pediatr* 1988;**113**:1022-7.
11) 下泉秀夫，岡部一郎，児玉浩子，柳沢正義．MRI で淡蒼球に病変を認めたメチルマロン酸血症の 1 例．脳と発達 1993;**25**:554-7.
12) Trinh BC, Melhem ER, Barker PB. Multi-slice proton MR spectroscopy and diffusion-weighted imaging in methylmalonic acidemia: report of two cases and review of the literature. *Am J Neuroradiol AJNR* 2001;**22**:831-3.
13) Toyoshima S, Watanabe F, Saido H, Miyatake K, Nakano Y. Methylmalonic acid inhibits respiration in rat liver mitochondria. *J Nutr* 1995;**125**:2846-50.
14) 内藤悦雄．母系遺伝性 Leigh 脳症．ミトコンドリアとミトコンドリア病．日本臨牀第 60 巻増刊号 4．大阪：日本臨牀社，2002:437-40.
15) 内藤悦雄．Leigh 脳症．「小児内科」「小児外科」編集委員会，共編．小児疾患診療のための病態生理 1．小児内科第 28 巻増刊号．東京：東京医学社，1996:753-5.
16) 高屋和志，吉岡 博，沢田 淳．MRS．「小児内科」「小児外科」編集委員会，共編．小児中枢神経疾患の画像診断．小児内科第 27 巻増刊号．東京：東京医学社，1995:189-95.
17) Koopmans RA, Li DK, Zhu G, Allen PS, Penn A, Paty DW. Magnetic resonance spectroscopy of multiple sclerosis: in-vivo detection of myelin breakdown products. *Lancet* 1993;**341**:631-2.

ELSEVIER

Brain & Development 26 (2004) 542–544

BRAIN & DEVELOPMENT
Official Journal of the Japanese Society of Child Neurology

www.elsevier.com/locate/braindev

Case report

Acute dysautonomia: complete recovery after two courses of IVIg

Mamiko Ishitobi*, Kazuhiro Haginoya, Taro Kitamura, Mitsutoshi Munakata, Hiroyuki Yokoyama, Kazuie Iinuma

Department of Pediatrics, Tohoku University School of Medicine, 1-1 Seiryo-machi, Aoba-ku, Sendai 980-8574, Japan

Received 17 June 2003; received in revised form 2 February 2004; accepted 24 February 2004

Abstract

An 11-year-old boy presented with acute dysautonomia manifesting as severe orthostatic hypotension following fever. Serial orthostatic tests with measurement of the coefficient of variation in the R–R intervals showed improvement after one course and complete recovery after two courses of intravenous high-dose immunoglobulin therapy (IVIg). Repeated courses of IVIg should be considered to treat this disorder if spontaneous remission does not occur.

Keywords: Acute dysautonomia; Orthostatic hypotension; Intravenous high-dose immunoglobulin therapy

Acute dysautonomia is a rare disorder, characterized by acute dysfunction of the autonomic nervous system with a history of preceding infection [1,2]. Acute dysautonomia has recently been recognized as a type of neuroimmunologic disorder. The pathogenesis remains unclear, but may involve acute inflammatory neuropathy caused by an immune mediated mechanism, similar to Guillain–Barré syndrome [2,3]. Recovery from acute dysautonomia tends to be gradual and frequently incomplete, and early therapeutic intervention is necessary in patients with progressive disability [1,2]. Acute dysautonomia has been successfully treated with intravenous high-dose immunoglobulin therapy (IVIg) [4–8]. We treated an 11-year-old boy who developed severe orthostatic hypotension after an episode of fever and recovered after two courses of IVIg.

1. Case report

A previously healthy 11-year-old boy developed high fever of 40 °C in September 2001 (Fig. 1). He complained of headache and dizziness at that time. His condition was treated as a common cold. The fever ceased 3 days later, but he suffered from sustained dizziness. Blood tests showed no abnormalities, but his blood pressure decreased from 88/46 mmHg to 68/42 mmHg at 4 min after standing. The diagnosis was orthostatic hypotension. He was treated with vasopressors, anti-inflammatory drugs, antidepressants, etc., but with no effect. Two months after the onset, he was referred to our hospital for further evaluation and treatment.

Serial measurements of the coefficient of variation in the R–R intervals (CVR–R) were made using a multi-function electrocardiograph (FDX-4520; Fukuda Denshi, Japan) during the orthostatic test monitored with a continuous non-invasive blood pressure tonometry system (JENTOW-7700; Colin Corporation, Japan). The orthostatic test was performed after resting for more than 15 min, and systolic and diastolic blood pressures were recorded every 10 to 15 s. The CVR–R was also measured at rest.

The orthostatic test demonstrated severe orthostatic hypotension (Fig. 2a). Immediately after standing, his heart rate suddenly rose to 140 beats/min, and his systolic blood pressure to higher than 140 mmHg. Seven minutes later, the systolic blood pressure sharply fell to lower than 80 mmHg, and he felt dizziness and loss of vision, and was unable to remain standing. He then lay down, but his heart rate and blood pressure did not recover to those measured before standing for 13 min. CVR–R was severely low at 2.05% (normal lower limit 3.0% in control subjects aged 10–19 years old) (Fig. 1).

He had a good appetite, and had no constipation or diarrhea. His hands were always cold and wet, but physical examination demonstrated no other abnormalities. He had no

* Corresponding author. Fax: +81-22-717-7290.
E-mail address: mamiko@ped.med.tohoku.ac.jp (M. Ishitobi).

0387-7604/$ - see front matter © 2004 Elsevier B.V. All rights reserved.
doi:10.1016/j.braindev.2004.02.012

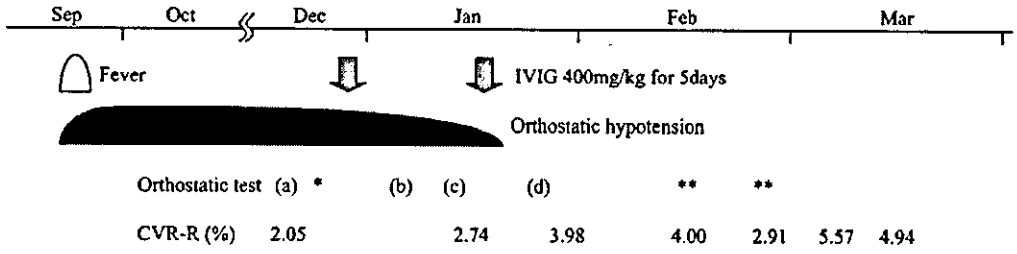

Fig. 1. Clinical course and timing of orthostatic tests and treatment. Coefficient of variation in the R–R intervals (CVR–R) showed gradual improvement after two courses of intravenous high-dose immunoglobulin therapy. As for orthostatic tests, * showed similar pattern to (a), and ** to (d). Refer to the results of orthostatic tests in Fig. 2.

vesicorectal problems. Neurological examination also demonstrated no abnormalities, including the cranial nerves, motor and sensory systems, and deep tendon reflexes. The ocular fundi were also normal. Motor and sensory nerve conducting velocities in the median nerves were within the normal range. Metaiodobenzylguanidine scintigraphy, which utilizes the noradrenaline analog metaiodobenzylguanidine for detection of autonomic dysfunction in the heart, showed no abnormalities. No abnormalities were found in blood and urine tests, including serum levels of antiganglioside antibodies. Cerebrospinal fluid (CSF) testing on admission showed normal levels of protein (18 mg/dl) and cell count (1/μl). Blood examination showed that immunoglobulin G antibody for human herpes virus 6 (HHV-6) was highly positive (1:160, normal < 1:10), and immunoglobulin M antibody for HHV-6 and polymerase chain reaction amplification of HHV-6 deoxyribonucleic acid were negative. Other virus antibody titers were negative.

The diagnosis was acute dysautonomia. He was treated with IVIg (400 mg/kg body weight for five consecutive

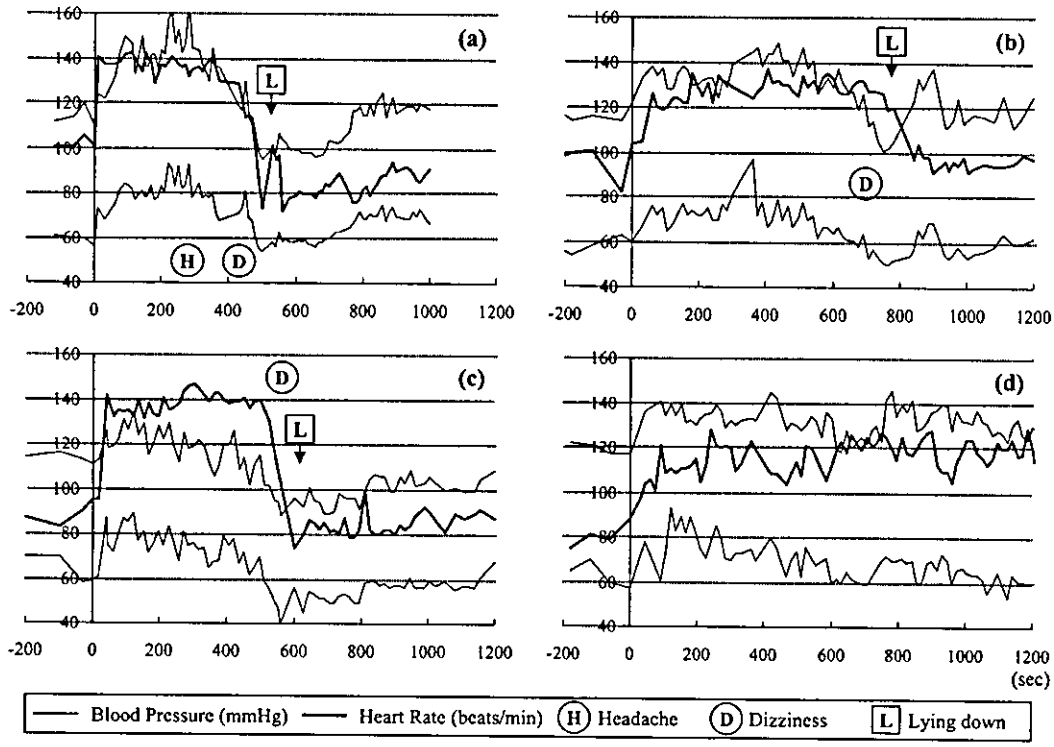

Fig. 2. Results of orthostatic tests. The timing of orthostatic tests was shown in Fig. 1. (a) Before treatment, the orthostatic test showed severe orthostatic hypotension, with sudden rises in blood pressure and heart rate immediately after standing, followed by impulsive falls in both 7 min after standing. Recovery of blood pressure and heart rate was poor after lying down. (b) The orthostatic test showed slight improvement after one course of intravenous high-dose immunoglobulin therapy, when he could remain standing for as long as 13 min. Changes in blood pressure and heart rate were less severe than before treatment, and recovery after lying down was prompt. (c) One week later, the orthostatic test showed a similar pattern to that before treatment. (d) The orthostatic test showed complete recovery after a second course of treatment.

days). The orthostatic test then showed his condition had slightly improved (Fig. 2b). He could remain standing for as long as 13 min. The changes in blood pressure and heart rate were less severe than before treatment, and recovery after lying down was prompt. However, one week later, the orthostatic test showed similar results to those before treatment (Fig. 2c), and CVR–R was still abnormally low at 2.74%. Another course of IVIg was given. The orthostatic test showed complete recovery (Fig. 2d) and the CVR–R returned to normal values (3.98%) (Fig. 1). He has had no complaints for more than one year.

2. Discussion

Acute dysautonomia can be considered as an uncommon variant of Guillain–Barré syndrome [5–8], because of the relatively common association of autonomic symptoms in Guillain–Barré syndrome, and because of the elevation of CSF protein in acute dysautonomia [6–8]. The level of CSF protein in our patient was normal, but the absence of any abnormality might be due to the late timing of the CSF examination, two months after the onset.

Our patient required two courses of IVIg to resolve his symptoms. The orthostatic test showed only slight improvement after the first course. Only one week later, the orthostatic test showed worsening of the symptoms and abnormally low CVR–R. However, temporary improvement was apparently observed after the first course, and a few reports have suggested that two courses of IVIg are necessary for effectiveness in cases of Guillain–Barré syndrome [9,10]. He showed complete and permanent recovery after the second course of treatment. The present case indicates that a second course of IVIg should be considered in patients with severe acute dysautonomia, especially if signs of improvement are observed after the first course.

Serial measurements of CVR–R and the orthostatic test using a tonometry system were useful for the evaluation of autonomic function in a child with acute dysautonomia. These methods are non-invasive and easy to carry out even in pediatric patients.

References

[1] Young RR, Asbury AK, Corbett JL, Adams RD. Pure pandysautonomia with recovery. Description and discussion of diagnostic criteria. Brain 1975;98:613–36.
[2] Suarez GA, Fealey RD, Camilleri M, Low PA. Idiopathic autonomic neuropathy: clinical, neurophysiologic, and follow-up studies on 27 patients. Neurology 1994;44:1675–82.
[3] Vernino S, Low P, Fealey RD, Stewar JD, Farrugia G, Lennon VA. Autoantibodies to ganglionic acetylcholine receptors in autoimmune autonomic neuropathies. N Engl J Med 2000;343:847–55.
[4] Heafield MT, Gammage MD, Nightingale S, Williams AC. Idiopathic dysautonomia treated with intravenous gammaglobulin. Lancet 1996; 347:28–9.
[5] Mericle RA, Triggs WJ. Treatment of acute pandysautonomia with intravenous immunoglobulin. J Neurol Neurosurg Psychiatry 1997; 62:529–31.
[6] Feldman EL, Bromberg MB, Blaivas M, Junck L. Acute pandysautonomic neuropathy. Neurology 1991;41:746–8.
[7] Quan D, Rich MM, Bird SJ. Acute idiopathic dysautonomia: electrophysiology and response to intravenous immunoglobulin. Neurology 2000;54:770–1.
[8] Meilof JF, Kwa VI, Vermeulen M, Tiessens G. Isolated ataxia and autonomic dysfunction: a new variant of Guillain–Barré syndrome? J Neurol Neurosurg Psychiatry 1998;64:689.
[9] Farcas P, Avnun L, Frisher S, Herishanu YO, Wirguin I. Efficacy of repeated intravenous immunoglobulin in severe unresponsive Guillain–Barré syndrome. Lancet 1997;350:1747.
[10] Ohtsuka T, Munakata M, Kato R, Yokoyama H, Haginoya K, Iinuma K, et al. A child with Guillain–Barré syndrome with successful treatment with two series of high-dose IVIG (in Japanese). Shonika Rinsho 2000;53:1819–23.

Epilepsia, 45(10):1248–1257, 2004
Blackwell Publishing, Inc.

Clinical Research

Dynamic Cortical Activity during Spasms in Three Patients with West Syndrome: A Multichannel Near-infrared Spectroscopic Topography Study

Mitsutoshi Munakata, Kazuhiro Haginoya, Mamiko Ishitobi, Osamu Sakamoto, Ikuko Sato, Taro Kitamura, Mieko Hirose, Hiroyuki Yokoyama, and Kazuie Iinuma

Department of Pediatrics, Tohoku University School of Medicine, Sendai, Japan

Summary: *Purpose:* To investigate spatial and temporal cortical activity during clusters of naturally occurring epileptic spasms in patients with West syndrome (WS) by using multichannel near-infrared spectroscopy (mNIRS).

Methods: Conventional magnetic resonance imaging (MRI) and interictal and ictal single-photon emission computed tomography (SPECT) were carried out in three patients with WS. Thereafter, cortical hemodynamics during naturally occurring epileptic spasms were measured by mNIRS with simultaneous video/electroencephalographic (EEG) monitoring.

Results: Ictal SPECT revealed multiple hyperperfused areas within the cortex. With the use of mNIRS, an increase in regional cerebral blood volume (CBV) was observed in these areas, which is representative of cortical activation. The increase in CBV was accompanied by an increase in the concentrations of both oxy- and deoxyhemoglobin. The following heterogeneous regional changes in CBV during ictus were observed: (a) transient increases that were synchronized with spasms; (b) a gradual increase during an ictal event that fluctuated in synchrony with spasms; and (c) a combination of transient and gradual increases. An increase in regional CBV occurred in multiple areas that were activated either simultaneously or sequentially during an ictal event. Topographic changes in CBV were closely correlated with the phenotype of the spasm.

Conclusions: During ictal events, multiple cortical areas were activated simultaneously or sequentially. The pattern of cortical activation closely affected the phenotype of the spasm, which suggested that the cortex was involved in the generation of spasms. **Key Words:** West syndrome—Infantile spasm—Near-infrared spectroscopy.

West syndrome (WS) is an age-dependent epileptic syndrome that occurs during infancy. WS is characterized by clustering epileptic spasms, electroencephalographic (EEG) hypsarrhythmia, and arrested psychomotor development (1,2). Although the pathophysiology of WS remains unknown, subcortical structures such as the lentiform nuclei and brainstem are thought to be involved (3,4). In addition, magnetic resonance imaging (MRI) and functional neuroimaging have revealed that a considerable number of children with WS possess focal cortical abnormalities (5–7). Surgical resection of the affected area can eliminate the spasms (8), suggesting (at least in such patients) that the abnormal cortex may play a crucial role in the pathogenesis of spasms in patients with WS.

Accepted June 6, 2004.
Address correspondence and reprint requests to Dr. M. Munakata at Department of Pediatrics, Tohoku University School of Medicine, 1-1 Seiryo-machi, Aoba-ku, Sendai 980-8574, Japan. E-mail: muna@ped.med.tohoku.ac.jp

Positron emission tomography (PET) and single-photon emission computed tomography (SPECT) have suggested that abnormal cortical areas are hyperperfused during ictal periods, implying that these areas of the cortex are activated during a cluster of spasms (9,10). However, because of the insufficient time resolution of PET and SPECT for rapidly progressing and repeatedly occurring spasms, it is impossible to discriminate between the cerebral perfusion changes during spasms and those at intervals of spasms, and postictal changes might contaminate the results. A different neuroimaging modality with superior time resolution is thus required to delineate the time course of cortical activity during the progression of the ictal events of WS.

Recently, multichannel near-infrared spectroscopy (mNIRS) has been used to investigate higher brain function because changes in regional cerebral blood volume (CBV), which can be measured by using mNIRS, are correlated closely with the topology of cortical activity (11,12). The relatively good time resolution of mNIRS

TABLE 1. *Clinical characteristics of patients*

	Case 1	Case 2	Case 3
Sex	female	female	male
Gestational age at birth (weeks)	35	37	40
Age (months)			
at onset	3	7	5
at examination	3	8	6
Seizure type	symmetrical spasms followed by asymmetrical spasms (L>R)	asymmetrical spasms (L>R) followed by symmetrical spasms	partial seizure followed by symmetrical spasms

overcomes the aforementioned limitation of PET and SPECT, and therefore it might be a useful method for observing spatial and temporal changes in cortical activity during ictus in patients with epilepsy (13). Here, we used mNIRS to assess the involvement of the cerebral cortex in ictal events in patients with WS.

METHODS

Patients

We studied three patients with WS. The clinical characteristics of the patients are summarized in Table 1.

Case 1

A girl (the first of twins) was born after 35 weeks of gestation; pregnancy and delivery were uncomplicated. The mother had Crohn's disease, but no family history of epilepsy was known. The first seizure occurred at age 3 months. During the ictal period, the girl exhibited brief extension of the upper and lower limbs, which was associated with upward rolling of the eyes. Initially, the spasms were symmetrical but became asymmetrical toward the end of a cluster in association with weak extension of the left upper limbs. An interictal EEG recording revealed hypsarrhythmia. The results of conventional MRI, retinal observation, and blood analyses (including lactate and amino acid analyses) were normal. Despite treatment for 2 weeks with vitamin B_6 and valproate (VPA), the infantile spasms remained. Although subsequent treatment with adrenocorticotropic hormone (ACTH) eliminated the spasms and the hypsarrhythmia, a brief tonic seizure without clustering occurred 1 month later.

Case 2

A girl was born after 37 weeks of gestation; pregnancy was uncomplicated. The first seizure was noted at age 7 months. During the ictal period, the girl exhibited brief spasms in clusters. Hypsarrhythmia was noted in an EEG recording. Vitamin B_6 and VPA were found to be ineffective, and she was referred to our hospital at age 8 months. MRI revealed a small lesion of unknown etiology at the posterior lateral aspect of the left lateral ventricle, whereas retinal observation and blood analyses were normal. Then ACTH treatment was carried out, and the spasms ceased, with an EEG improvement.

Case 3

A boy was born after 40 weeks of gestation; pregnancy was uncomplicated. The first seizure was noted at age 5 months. During the ictal period, he exhibited brief extension of the upper limbs with head-nodding. At age 6 months, he could no longer control the movements of his head, and he was referred to our hospital. Hypsarrhythmia was noted in an interictal EEG. The MRI, retinal observation, and metabolic parameters were normal. ACTH treatment was carried out after vitamin B_6 and VPA were found to be ineffective. After the ACTH treatment, the hypsarrhythmia disappeared, and the spasms ceased.

Methods

Within 2 weeks of admission to the Tohoku University Hospital and before the initiation of ACTH therapy, interictal and ictal SPECT and ictal mNIRS with video-EEG monitoring were carried out in each of the three aforementioned patients. We received informed consent from the parents of the patients for the following examinations.

For ictal SPECT, as soon as the attending pediatrician noticed the occurrence of spasms, [^{99m}Tc]-ethyl cysteinate dimer (ECD) was injected intravenously. The fixation of [^{99m}Tc]-ECD within the brain after injection required several minutes (14). Because multiple spasms occurred during this period, the SPECT images obtained represented mixed cerebral blood flow (CBF) during the multiple spasms. For the interictal SPECT study, [^{99m}Tc]-ECD was injected while the patient was conscious. Both ictal and interictal SPECT images were acquired at 30 min after the injection of [^{99m}Tc]-ECD by using a MULTI-SPECT 3 (Siemens, Gerfahldt, Germany). The patient was sedated with diazepam (DZP) during the scanning. The method that we used to construct a tomogram of CBF has been described elsewhere (10).

NIRS is based on the fact that near-infrared light can propagate through biologic material with scattering, and the absorption during propagation is inversely related to hemoglobin (Hb) concentrations in tissues (15). By using two specific wavelengths of near-infrared light (see later), the relative changes in oxy- and deoxy-Hb concentrations can be calculated separately (11). The summation of oxy- and deoxy-Hb concentrations gives the change in total Hb (total-Hb) concentrations, which is representative of changes in CBV (16).

In the present study, a mNIRS system (ETG 100; Hitachi Medical Corporation, Tokyo, Japan) was used. After the placement of selected scalp electrodes for digital EEG monitoring (EEG2100; Nihon Kohden, Tokyo, Japan), two optode arrays for mNIRS were fixed to the scalp by using a tubular net bandage and surgical tape. Based on the SPECT results, the arrays were placed bilaterally symmetrically with the center of each array located approximately

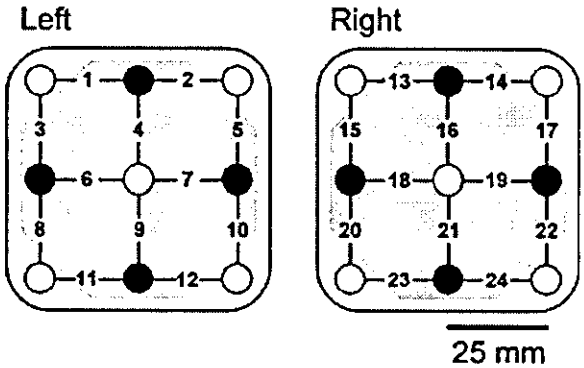

FIG. 1. Configuration of optode arrays. Each array consisted of alternately arranged light-emitting (*solid circles*) and light-detecting (*open circles*) optodes. Absorption of near-infrared light (780 and 840 nm) was measured among adjoining emitting and detecting optodes, thereby producing 12 recording channels per hemisphere (channels 1–12, right hemisphere; 13–24, left hemisphere). The gray area illustrates the extent of the topographic image that was constructed by using spatial spline interpolation across the recording channels.

over the frontal or central area (10-20 system). The attachment for the arrays was fabricated specifically for infants to minimize discomfort (Hitachi Medical Corporation). Each array comprised four light-emitting and five light-detecting optodes that were arranged alternately with a spacing of 25 mm (Fig. 1). The absorption of backscattered light at wavelengths of 780 and 840 nm was measured between adjoining optodes, thereby producing 12 measurement channels per hemisphere. The sampling interval was 0.5 s. For off-line analysis, baseline values of oxy-, deoxy-, and total-Hb were aligned to the period that immediately preceded the ictal period (unless otherwise stated). Topographic images of the changes in regional CBV were constructed by using spline interpolation. The spatial resolution of the images was limited by interoptode distance.

RESULTS

Figure 2A shows the results of the interictal (Fig. 2A, a–d) and ictal SPECT (Fig. 2A, e–h) for case 1. During ictus, a prominent increase in regional CBF was noted in the right anterior frontal lobe (arrow in Fig. 2A, e), which was surrounded by a relatively hypoperfused area (arrowhead). The contralateral cortex also was hyperperfused with a predominant increase in regional CBF in the left frontal area (Fig. 2A, e and f). In addition, an increase in regional CBF during ictus was observed in subcortical structures such as the bilateral lentiform nuclei, cerebellum, and brainstem (Fig. 2A, g and h).

In case 1, 19 spasms were recorded during mNIRS monitoring. Figure 2B shows representative topographic maps of the spatial changes in total-Hb concentrations (which reflect regional changes in CBV) in the bilateral frontal area during spasms. A focal increase in CBV occurred in the right hemisphere, whereas a simultaneous decrease in CBV occurred in the adjacent area. In the left hemisphere, CBV increased in a relatively diffuse manner. Figure 2C, a and b, illustrate the time course of changes in total-, oxy-, and deoxy-Hb concentrations during a cluster of spasms in the right hemisphere at the channels indicated by (a) and (b) in Figure 2B. In Figure 2C, a, the increase in regional CBV was transient, and the increase was synchronized with the spasm (arrowheads). In addition, a peripheral decrease in CBV (Fig. 2C, b) also was synchronized with the spasm. The first 11 spasms were intensely tonic and symmetrical (solid arrowheads in Fig. 2C); thereafter, the spasms became weak and asymmetrical (open arrowheads), and the spasms were associated with extension of the left arm. Intense spasms tended to be correlated with high total-Hb concentrations.

Figure 2D shows representative ictal EEG recordings during a spasm. A focal spike in the right hemisphere preceded each spasm. After this, fast waves occurred with right-hemisphere dominance; these waves were superimposed with high-voltage slow waves and were followed by desynchronization. The dotted line in Figure 2D indicates the onset of the spasm as determined by surface electromyography (EMG).

Figure 3A shows the results of interictal (Fig. 3A, a–d) and ictal (Fig. 3A, e–h) SPECT for case 2. During ictus, a bilateral increase in regional CBF was observed in the parietooccipital cortex, along with an increase in regional CBF in the bilateral lentiform nuclei. Consequently, for case 2, the optode arrays for mNIRS were placed symmetrically bilaterally, with the center of each array located over the central area (10-20 system), as illustrated in the insets in Figure 3B.

Figure 3B shows topographic maps of the regional CBV changes around the right and left central areas during a spasm for case 2 at the time point indicated by an asterisk in Figure 3C. A focal increase in CBV was seen in the posterior region of the right topographic map. A slight increase in CBV was observed also in the left homologous site. Figure 3C shows the time course of changes in total-, oxy-, and deoxy-Hb concentrations during a cluster of spasms in the right (R) and left (L) hemispheres at the same points in the corresponding hemispheres (solid circles in Fig. 3B). The spasms gradually became more intense during the progression of a cluster, and continuous recording in the right hemisphere became impossible after the eighth spasm, owing to the development of intense motion (broken line in Fig. 3C). Initially, the transient increase in CBV was synchronized with spasms in the right hemisphere; thereafter, a periodic increase in CBV in the left hemisphere gradually became obvious.

Figure 3D, a–c, shows an ictal EEG and surface EMG recordings that were made at the bilateral deltoid muscle;

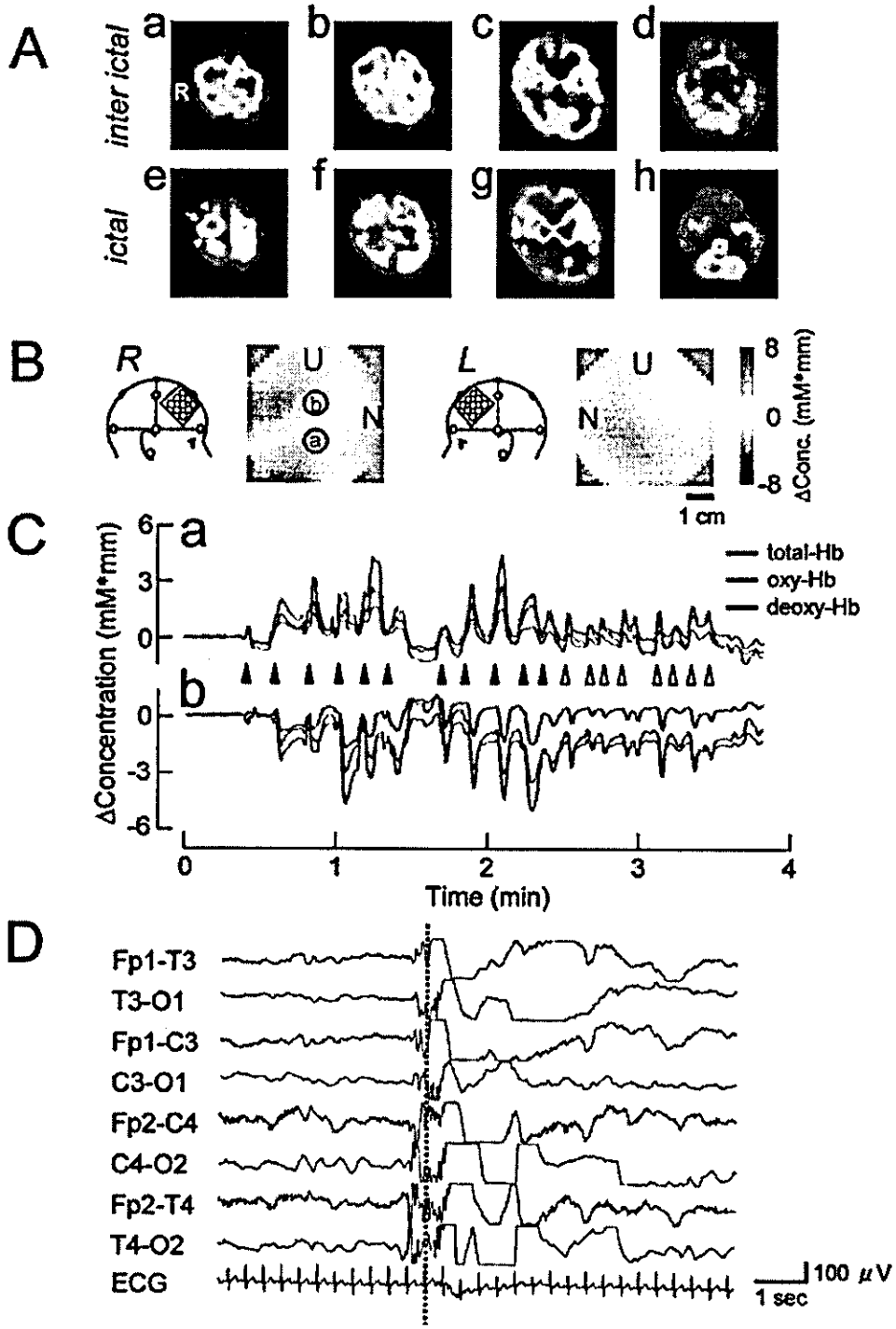

FIG. 2. Results for case 1. **A:** Results of [^{99m}Tc]-ethyl cysteinate dimer (ECD) single-photon emission computed tomography (SPECT) during interictal and ictal periods. Displays are transverse SPECT images parallel to the orbitomeatal plane that were obtained during interictal (a–d, in order from top to bottom of brain) and ictal (e–h) periods. The *arrow* and *arrowheads* in panel e indicate a hyper- and hypoperfused area of cortex, respectively. R, right. **B:** Representative topographic changes in regional cerebral blood volume (CBV) as inferred from changes in total hemoglobin (Hb) concentrations during spasms. U, upper; N, nasal. Insets illustrate the placement of the optode arrays and electroencephalography (EEG) electrodes. R, right, L, left. The time course of changes in ictal Hb concentrations at the recording channels that are indicated by ⓐ and ⓑ in B, are shown in panels Ca and b, respectively. **C:** The time course of changes in oxy-, deoxy-, and total-Hb concentrations at the points indicated by ⓐ and ⓑ in **B** are illustrated in panels Ca and b, respectively. *Arrowheads,* the occurrence of spasms. Initially, spasms were symmetrical (*solid arrowheads*), and were followed by asymmetrical, weak spasms in the left upper limbs (*open arrowheads*). **D:** Ictal EEG recorded simultaneously with multichannel near-infrared spectroscopy (mNIRS). The *broken line* indicates the onset of a spasm.

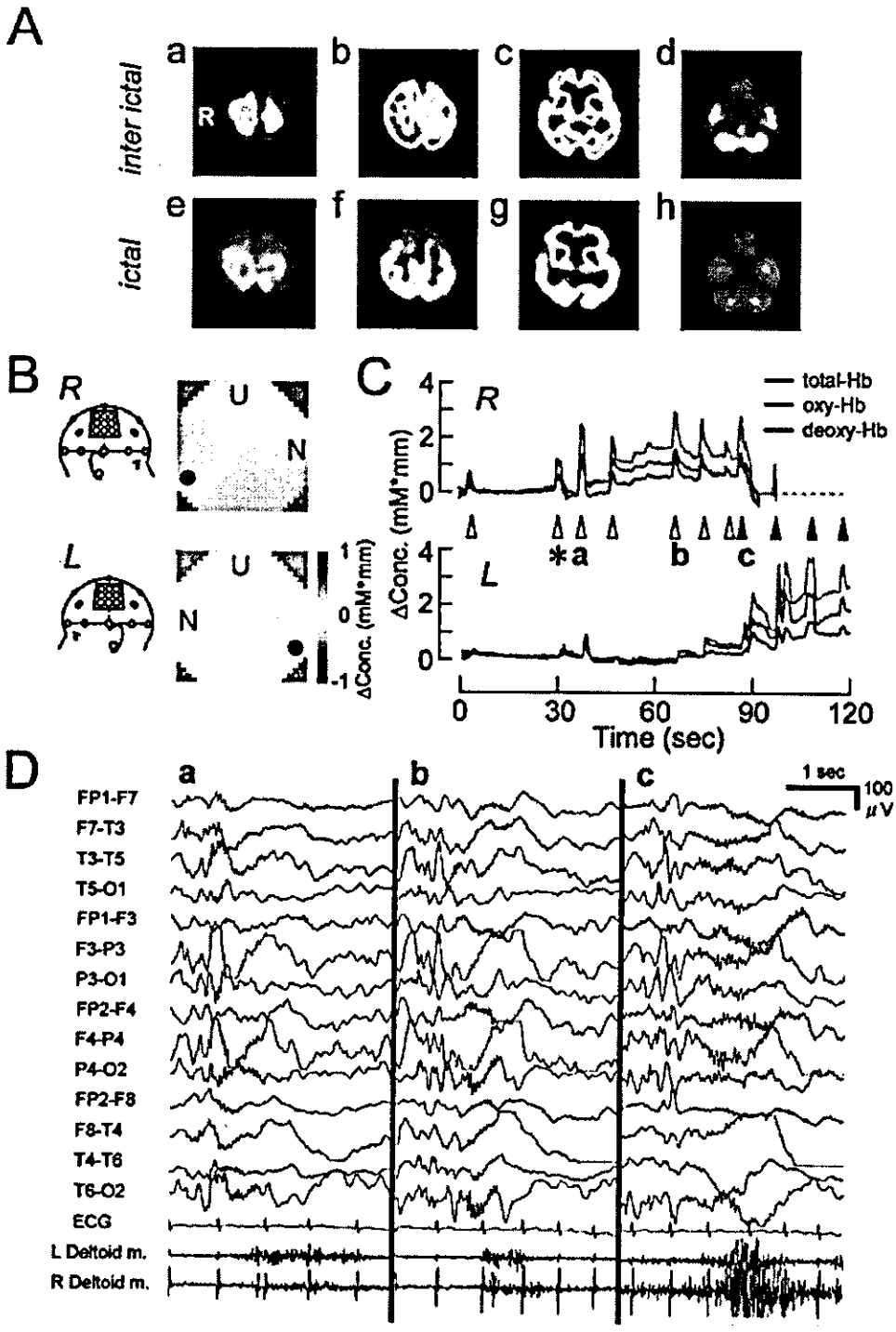

FIG. 3. Results for case 2. **A:** Results of SPECT during interictal (a–d) and ictal (e–h) periods. **B:** Topographic changes in cerebral blood volume (CBV; total-Hb concentrations) during a spasm. Insets illustrate the location of the optode arrays. The *solid circles* indicate the sites at which changes in Hb concentrations are illustrated in **C. C:** The time course of changes in Hb concentrations at the points is indicated by the solid circles in **B**. *Arrowheads*, The occurrence of spasms. Spasms were initially weak (*open arrowheads*), and subsequently transformed into massive tonic spasms (*solid arrowheads*) that prevented stable recording from the right hemisphere (*dashed line*). *Time at which the topographic changes in CBV are depicted in **B. D:** Ictal EEG during spasms. Panels a–c correspond to the spasms indicated by a–c in **C**. Initially, short discharges of fast waves occurred predominantly in the right hemisphere. A surface EMG revealed that the spasm in the left hemisphere occurred earlier and was more intense than that in the right hemisphere (a). Thereafter, fast waves became evident in the left hemisphere during the progression of the ictus (b, c), and intensity of spasms increased in the right hemisphere. Note that the laterality of regional changes in CBV was closely correlated with the fast waves and the intensity of the spasms.

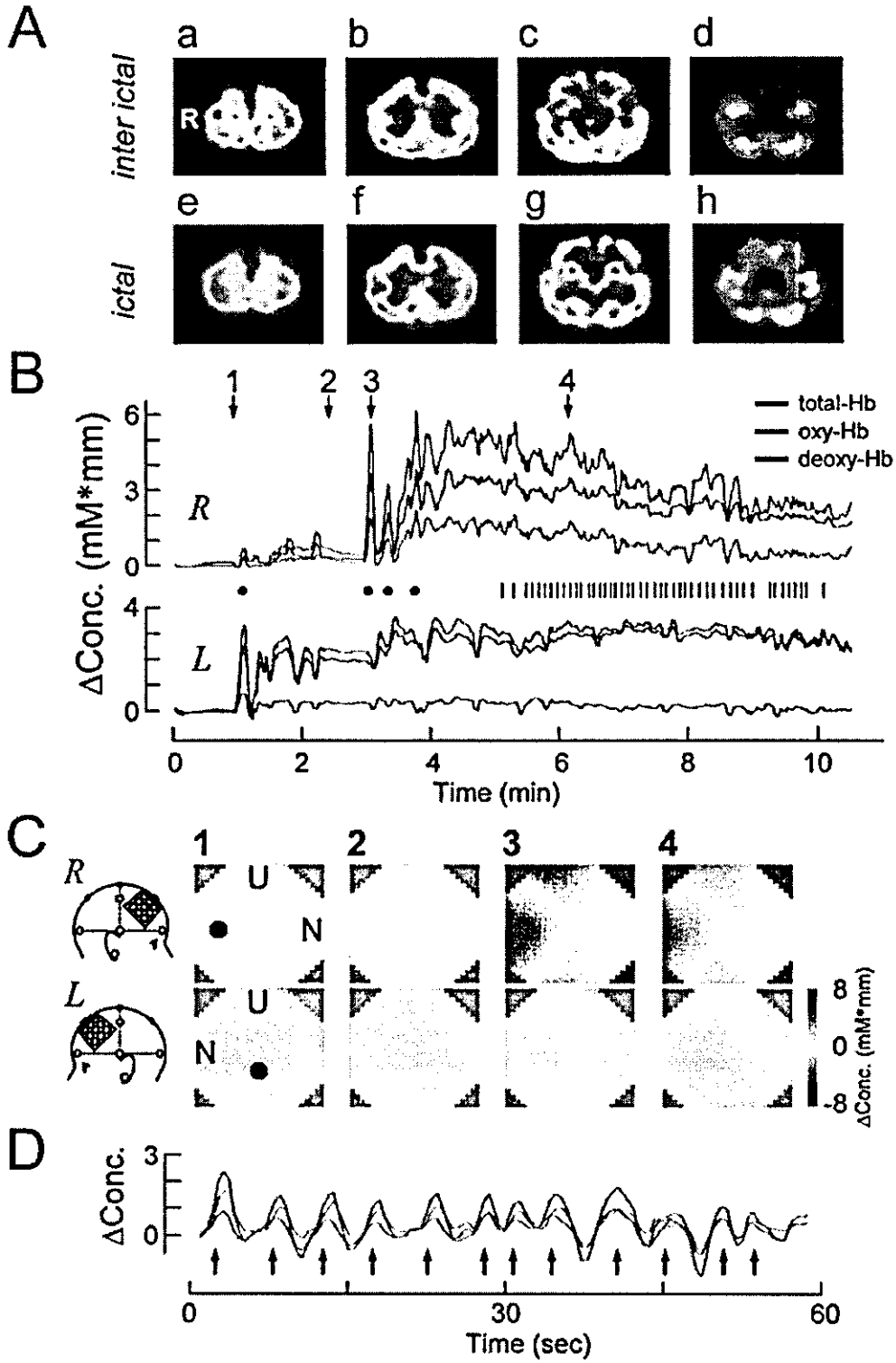

FIG. 4. Results for case 3. **A.** Results of SPECT during interictal (a–d) and ictal periods (e–h). **B.** The time course of changes in Hb concentrations at the points indicated by the *solid circles* in **C.** During the ictal period, atypical slight truncal movement was observed initially (*solid circles*), after which weak spasms occurred frequently (vertical bars). Topographic changes in cerebral blood volume (CBV) at the times corresponding to numbers 1–4 are illustrated in **C. C:** Topographic changes in CBV at the times indicated by numbers 1–4 in **B. D:** The time course of changes in Hb concentrations at the points indicated by the solid circles in **C***R* for a different ictal event are shown on an expanded time scale. Traces depicting oxy-, deoxy-, and total-Hb concentrations were realigned to time 0. *Arrows,* The occurrence of spasms. Concentrations of oxy-, deoxy-, and total-Hb fluctuated in concert with the occurrence of the spasms.

the corresponding times for the mNIRS data are indicated in Figure 3C, a–c. As noted in the surface EMG, initially spasms occurred slightly earlier in the left side of the body; thereafter, spasms occurred simultaneously in both sides.

Figure 4A shows the results of interictal (Fig. 4A, a–d) and ictal (Fig. 4A, e–h) SPECT for case 3. During ictus, an increase in regional CBF occurred in the right parietofrontal cortex, along with increases in regional CBF in subcortical structures. The interictal EEG during sleep for case 3 revealed symmetrical hypsarrhythmia (Fig. 5A). About 4 minutes before the initiation of clinically obvious spasms, case 3 awoke, and the hypsarrhythmia became irregular slow waves. Thereafter, a diffuse high-voltage slow wave that was led by the left hemisphere was noted, and this was followed by theta waves in the same hemisphere (Fig. 5B). At this time, slight truncal movement occurred (arrow in Fig. 5B). In the corresponding time period, a sudden increase in regional CBV occurred in the left hemisphere (number 1 in Fig. 4B and C), which was sustained. In the EEG (Fig. 5C), the theta activity became rhythmic and was observed bilaterally with an increased spike frequency in the right midtemporal area. During this period, a slight increase in regional CBV was noted in the right hemisphere (number 2 in Fig. 4B and C), and the patient did not exhibit any movement. Thereafter, a focal increase in regional CBV occurred suddenly several times in the right hemisphere (number 3 in Fig. 4B and C), which was accompanied by atypical slight truncal movement. The truncal movement was considered to be an ictal phenomenon, because a high-voltage slow wave was noted in the EEG that was recorded at the same time (Fig. 5D). Thereafter, a gradual focal increase in regional CBV was seen in the right hemisphere, which reached a maximum value at which weak but clinically obvious spasms occurred (short vertical bars in Fig. 4B). The spatial distribution of the gradual increase in CBV is shown in Fig. 4C. The corresponding ictal EEG comprised diffuse small fast waves that were followed by a slow wave (Fig. 5E). Figure 4D shows the changes in regional CBV that were recorded from the same channel in the right hemisphere as that depicted in Figure 4C (solid circle) during a different cluster of spasms in the same patient at a magnified time scale. Fluctuations in total-, oxy-, and deoxy-Hb concentrations were synchronized with the spasms.

DISCUSSION

In the present study, we used mNIRS to measure ictal changes in regional CBV during naturally occurring

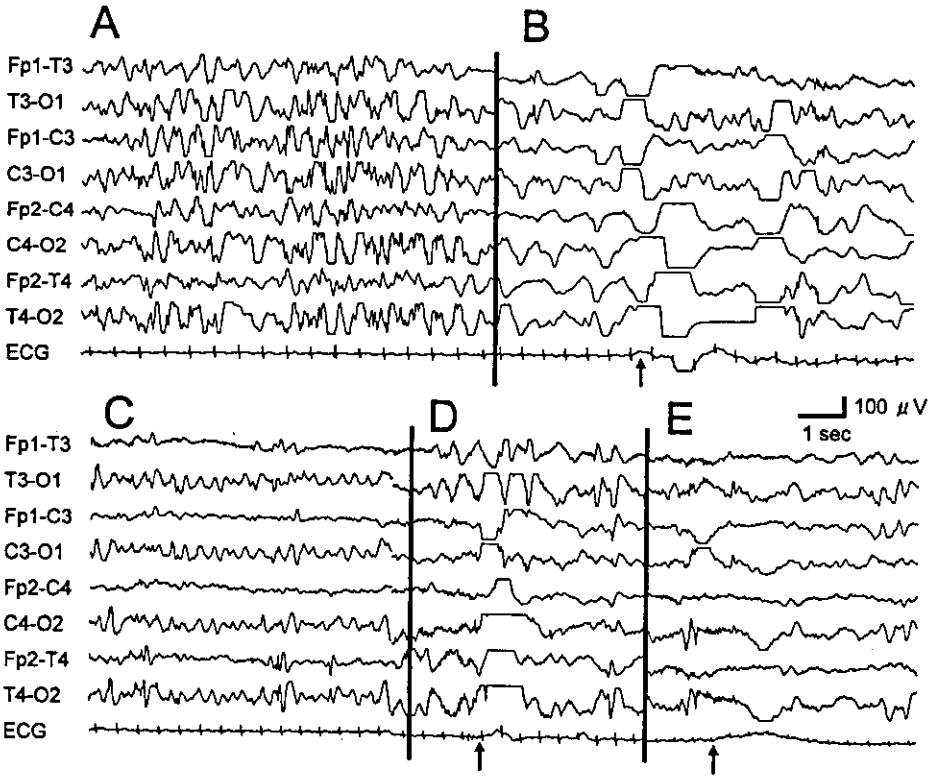

FIG. 5. Interictal and ictal EEG for case 3. **A:** Interictal EEG showing hypsarrhythmia. **B:** Approximately 4 min after the attenuation of hypsarrhythmia, atypical truncal movement was noted, and focal rhythmic theta discharges emerged in the left occipital area. **C:** The theta discharge propagated to the right hemisphere, and an increase in the number of spikes was seen around recording channel T4. **D:** The theta activity changed to high-voltage slow waves, and atypical truncal movement occurred again. **E:** Ictal movement became a typical tonic spasm. *Arrows* in **B**, **D**, and **E** indicate the occurrence of ictal events (atypical movements or spasms), as determined by video-recording the patient during the EEG monitoring.

spasms in patients with WS. Considering the multiple etiologies (1) and heterogeneity of cortical involvement in WS (5,10), limited scope exists for the generalization of our observations. Nevertheless, our results have revealed some remarkable properties of the dynamic nature of cortical activity during epileptic spasms.

Intracranial propagation of near-infrared light is affected by multiple age-dependent factors, such as the optical properties of the scalp, skull, cerebrospinal fluid, and brain. In the adult head, the propagation of light through the brain is largely confined to the cortical gray matter, whereas in the neonatal head, light passes mainly through the cortex, although light may penetrate the subcortical white matter (17,18). Although subcortical structures, especially the lentiform nuclei, were activated during the ictal period in the present cases, the concomitant absorption change in such the deep brain areas was thought to be small with the short interoptode distance in the present study (18). However, further investigation is required to clarify how intracranial propagation of light changes with age.

Experiments using mNIRS have revealed that a tight coupling exists between hemodynamics and neuronal activity in the cortex. Habitual tasks or physiological stimuli evoke a focal increase in CBV (total-Hb concentrations) within a functionally corresponding area of the cortex (11,12). The increase in CBV is a result of the dilatation of regional microvessels, which is regulated locally by astrocytes that respond to neuronal activation (19). Because the activity-dependent CBV increase is much greater than the local oxygen demand, the change in CBV is usually accompanied by an increase in oxy-Hb concentrations, whereas deoxy-Hb concentrations decrease (20,21). Although ictal cortical hemodynamics are heterogeneous among the types of seizure, an increase in CBV together with an increase in both oxy- and deoxy-Hb concentrations has been noted during generalized convulsive seizures (22,23). The increase in deoxy-Hb concentrations is thought to reflect large oxygen consumption, implying the presence of intense neuronal activation. However, activity-related changes in deoxy-Hb concentrations may be modified by maturation processes in cerebral hemodynamics: normal adults tend to show a decrease in deoxy-Hb concentrations during physiological stimuli, whereas young infants tend to exhibit an increase in deoxy-Hb concentrations (24,25). In patients with WS, CBV increased with a marked increase in deoxy-Hb concentrations. Although the increase in deoxy-Hb concentrations suggests an expansion in oxygen consumption during intense epileptic cortical discharges, cerebral immaturity may affect the extent of the increase in deoxy-Hb concentrations in infants.

The use of mNIRS in the present study revealed that regional changes in CBV during the ictal period were highly dynamic and were distributed focally. We were able to identify three different patterns of regional increases in CBV: (a) repetitive transient increases that were synchronized with spasms (these were observed in case 1); (b) a gradual fluctuating increase during a cluster that was synchronized with spasms (case 3); and (c) a periodic transient increase that also contained elements that resembled a gradual increase (case 2). The ictal short discharges of fast waves, which were prominent in cases 1 and 2, might be the events within the EEG recordings that were associated with a transient increase in regional CBV. The fast waves occurred immediately before the onset of each spasm and were the result of focal cortical discharges, which are thought to give rise to the spasms (26,27). In cases 1 and 2, a transient increase in CBV began immediately before a spasm, at the time at which fast waves emerged. The intensity and laterality of the increase in regional CBV was correlated with the amplitude of the fast waves. Therefore we believe that a focal transient increase in regional CBV reflects the ictal cortical discharge that produces fast waves.

The pathophysiologic basis for the gradual increase in CBV during a cluster of spasms remains unknown. One explanation is that gradual increases in CBV might be indicative of the presence of an epileptogenic area that is activated subclinically before the spasms, which subsequently dominates the entire ictal event. Previous clinical studies using single-channel NIRS reported the preictal hemodynamic change in pediatric cases with generalized seizures and with WS (23,28). The progressive increase in CBV may result from frequent periodic or sustained cortical discharge, which might in turn cause an accumulation of blood. Alternatively, it is possible that the gradual increase in CBV resulted from the combined activity of simultaneously progressing partial seizures (29), rather than from spasms, and that the increase in CBV masked an initial transient increase. To elucidate the involvement of the aforementioned pathophysiologic mechanisms, further investigations using more advanced mNIRS (e.g., a wider recording area and greater spatial resolution) are required.

In the area surrounding the region of largely increased CBV, a decrease in regional CBV was found that might have corresponded to the hypoperfused area that was noted in the ictal SPECT. The decrease in regional CBV occurred repeatedly with each spasm, suggesting that this was neither ictal exhaustion nor a postictal decrease in regional CBF, which is observed in other types of epilepsy (30). The decrease in regional CBV was caused predominantly by a change in the concentration of oxy-Hb, which suggests that the arterial blood supply was reduced; this might indicate the existence of a local steal phenomenon (31).

In the present study, mNIRS revealed that ictal cortical activation occurred in multiple cortical regions that were activated simultaneously or sequentially during the

progression of an ictal event. In cases 1 and 2, bilateral homologous sites were activated, whereas in case 3, unilateral cortical discharge that caused a partial seizure appeared to facilitate contralateral cortical activation that resulted in a single ictal event (24). Although single unilateral cortical discharges lead to bilateral spasms, presumably via subcortical structures (32), the pattern of activation of multiple cortical areas might affect the laterality and intensity of spasms. The mechanism by which multiple cortical areas interact during an ictal event is not known. Pinard et al. (33) reported that complete corpus callosotomy of a patient with WS resulted in asymmetrical spasms and unilateral hypsarrhythmia, and they suggested that the secondary generalization might have been caused by transcallosal propagation. Alternatively, it is possible that subcortical structures mediate such cortical interaction (2).

The analysis of changes in regional CBV in the present study suggested that spasms might have originated within the cortex in the present cases. However, it is unlikely that focal cortical activation generated the spasms autonomously, because the spasms were bilaterally tonic and repetitive, and ictal SPECT revealed symmetrical hyperperfusion of subcortical structures. It is likely that subcortical structures are involved in the propagation of spasms (9,10). Thus cortical activation may subsequently activate the subcortical effectors that ultimately produce spasms. Nevertheless, it should be noted that a possibility exists that subcortical primary lesions can cause epileptic spasms in some WS patients (23,34). If so, the properties of spasms in WS patients may be the result of a mutual interaction between cortical and subcortical structures via an unknown, age-dependent mechanism (2).

In conclusion, dynamic ictal cortical activity was recorded during clusters of spasms by using mNIRS. During ictal events, multiple cortical areas were activated simultaneously or sequentially. The pattern of cortical activation strongly influenced the phenotype of the infantile spasm, which suggested that the cortex was involved in the generation of spasms. Finally, the results of the present study exemplify how mNIRS can provide useful information in studies of seizure semiology.

REFERENCES

1. Watanabe K. West syndrome: etiological and prognostic aspects. *Brain Dev* 1998;20:1–8.
2. Dulac O. What is West syndrome? *Brain Dev* 2001;23:447–52.
3. Fukuyama Y, Shionaga A, Iida Y. Polygraphic study during whole night sleep in infantile spasms. *Eur Neurol* 1979;18:302–11.
4. Chugani HT, Shewmon DA, Sankar R, et al. Infantile spasms, II: lenticular nuclei and brain stem activation on positron emission tomography. *Ann Neurol* 1992;31:212–9.
5. Chugani HT, Shields WD, Shewmon DA, et al. Infantile spasms, I: PET identifies focal cortical dysgenesis in cryptogenic cases for surgical treatment. *Ann Neurol* 1990;27:406–13.
6. Metsähonkala L, Gaily E, Rantala H, et al. Focal and global cortical hypometabolism in patients with newly diagnosed infantile spasms. *Neurology* 2002;58:1646–51.
7. Chiron C, Dulac O, Bulteau C, et al. Study of regional cerebral blood flow in West syndrome. *Epilepsia* 1993;34:707–15.
8. Asano E, Chugani DC, Juhasz C, et al. Surgical treatment of West syndrome. *Brain Dev* 2001;23:668–76.
9. Chugani HT, Rintahaka PJ, Shewmon DA. Ictal patterns of cerebral glucose utilization in children with epilepsy. *Epilepsia* 1994;35:813–22.
10. Haginoya K, Munakata M, Yokoyama H, et al. Mechanism of tonic spasms in West syndrome viewed from ictal SPECT findings. *Brain Dev* 2001;23:496–501.
11. Maki A, Yamashita Y, Ito Y. Spatial and temporal analysis of human motor activity using noninvasive NIR topography. *Med Phys* 1995;22:1997–2005.
12. Watanabe E, Maki A, Kawaguchi F, et al. Non-invasive assessment of language dominance with near-infrared spectroscopic mapping. *Neurosci Lett* 1998;256:49–52.
13. Watanabe E, Nagahori Y, Mayanagi Y. Focus diagnosis of epilepsy using near-infrared spectroscopy. *Epilepsia* 2002;43(suppl 9):50–5.
14. Holman BL, Hellman RS, Goldsmith SJ, et al. Biodistribution, dosimetry, and clinical evaluation of technetium-99m ethyl cysteinate dimer in normal subjects and in patients with chronic cerebral infarction. *J Nucl Med* 1989;30:1018–24.
15. Jöbsis FF. Noninvasive, infrared monitoring of cerebral and myocardial oxygen sufficiency and circulatory parameters. *Science* 1977;198:1264–7.
16. Wyatt JS, Cope M, Delpy DT, et al. Quantitation of cerebral blood volume in human infants by near-infrared spectroscopy. *J Appl Physiol* 1990;68:1086–91.
17. Faris F, Thorniley M, Wickramasinghe Y, et al. Non-invasive in vivo near-infrared optical measurement of the penetration depth in the neonatal head. *Clin Phys Physiol Meas* 1991;12:353–8.
18. Fukui Y, Ajichi Y, Okada E. Monte Carlo prediction of near-infrared light propagation in realistic adult and neonatal head models. *Appl Opt* 2003;42:2881–7.
19. Anderson CM, Nedergaard M. Astrocyte-mediated control of cerebral microcirculation. *Trends Neurosci* 2003;26:340–4.
20. Kato T, Kamei A, Takashima S, et al. Human visual cortical function during photic stimulation monitoring by means of near-infrared spectroscopy. *J Cereb Blood Flow Metab* 1993;13:516–20.
21. Obrig H, Wolf T, Doge C, et al. Cerebral oxygenation changes during motor and somatosensory stimulation in humans, as measured by near-infrared spectroscopy. *Adv Exp Med Biol* 1996;388:219–24.
22. Sokol DK, Markand ON, Daly EC, et al. Near infrared spectroscopy (NIRS) distinguishes seizure types. *Seizure* 2000;9:323–7.
23. Haginoya K, Munakata M, Kato R, et al. Ictal cerebral haemodynamics of childhood epilepsy measured with near-infrared spectrophotometry. *Brain* 2002;125:1960–71.
24. Meek JH, Firbank M, Elwell CE, et al. Regional hemodynamic responses to visual stimulation in conscious infants. *Pediatr Res* 1998;43:840–3.
25. Yamada H, Sadato N, Konishi Y, et al. A rapid brain metabolic change in infants detected by *f*MRI. *Neuroreport* 1997;8:3775–8.
26. Panzica F, Franceschetti S, Binelli S, et al. Spectral properties of EEG fast activity ictal discharges associated with infantile spasms. *Clin Neurophysiol* 1999;110:593–603.
27. Watanabe K, Negoro T, Okumura A. Symptomatology of infantile spasms. *Brain Dev* 2001;23:453–66.
28. Adelson PD, Nemoto E, Scheuer M, et al. Noninvasive continuous monitoring of cerebral oxygenation periictally using near-infrared

spectroscopy: a preliminary report. *Epilepsia* 1999;40:1484–9.
29. Donat JF, Wright FS. Simultaneous infantile spasms and partial seizures. *J Child Neurol* 1991;6:246–50.
30. Zubal IG, Spanaki MV, MacMullan J, et al. Influence of technetium-99m-hexamethylpropylene amine oxime injection time on single-photon emission tomography perfusion changes in epilepsy. *Eur J Nucl Med* 1999;26:12–7.
31. Lee HW, Hong SB, Tae WS. Opposite ictal perfusion patterns of subtracted SPECT: hyperperfusion and hypoperfusion. *Brain* 2000;123:2150–9.
32. Haginoya K, Kon K, Tanaka S, et al. The origin of hypsarrhythmia and tonic spasms in West syndrome: evidence from a case of porencephaly and hydrocephalus with focal hypsarrhythmia. *Brain Dev* 1999;21:129–31.
33. Pinard JM, Delalande O, Chiron C, et al. Callosotomy for epilepsy after West syndrome. *Epilepsia* 1999;40:1727–34.
34. Desguerre I, Pinton F, Nabbout R, et al. Infantile spasms with basal ganglia MRI hypersignal may reveal mitochondrial disorder due to T8993G MT DNA mutation. *Neuropediatrics* 2003;34:265–9.

Seizure (2004) 13S, S34–S39

ELSEVIER

SEIZURE

www.elsevier.com/locate/yseiz

Clinical efficacy of zonisamide in childhood epilepsy after long-term treatment: a postmarketing, multi-institutional survey

Kazuie Iinuma*, Kazuhiro Haginoya

Department of Pediatrics, Tohoku University School of Medicine, 1-1 Seiryo-machi, Aoba-ku, Sendai, Miyagi 980-8574, Japan

KEYWORDS
Zonisamide;
Epilepsy;
Japan;
Pediatric;
Efficacy

Summary Postmarketing data about the effectiveness of zonisamide in childhood epilepsy was collected from 759 children with various forms of epilepsy (ages 3 months–15 years) to compare the long-term efficacy of zonisamide in the treatment of epilepsy in intellectually normal versus intellectually disabled children. The follow-up period was 6 months–3 years; 291 children (245 intellectually normal, 46 intellectually disabled) received zonisamide as monotherapy. The remaining patients received additional antiepilepsy drugs (AEDs); mean numbers of additional AEDs were 1.6 and 2.9 for intellectually normal and intellectually disabled groups, respectively. Effectiveness could not be evaluated in 30 of the 759 patients because of very rare or irregular seizure frequency. In the 729 patients evaluated, 78% of intellectually normal patients and 43% of intellectually disabled patients showed ≥50% reduction in the number of seizures ($P < 0.001$). Improvement rates seen in the intellectually normal group were almost the same for patients with generalized (82%) and partial (77%) epilepsies, whereas in the intellectually disabled group, the improvement rate was higher for partial (50%) than generalized (36%) epilepsies ($P < 0.01$).

These results are consistent with the known phenomenon that intellectually disabled children are likely to have more intractable seizures than children with normal intelligence.

Introduction

Zonisamide is a new drug with broad-spectrum antiepilepsy activity against partial as well as generalized seizures. The drug has been commercially licensed in Japan since 1989. Before licensure, randomized, controlled trials of zonisamide were performed by 4 authors;[1–4] 3 studies were of treatment in adults,[1–3] and 1 study examined pediatric treatment.[4] The observation period of these studies was 12–16 weeks in adults, and 8 weeks in children. All studies were confined to zonisamide treatment of generalized seizures. Postmarketing research, performed at 25 institutions over a 5-year period, investigated the clinical effectiveness and safety of zonisamide for the treatment of childhood epilepsy. The purpose of this postmarketing study was to compare the long-term efficacy of zonisamide in the treatment of epilepsy in intellectually nor-

*Corresponding author. Tel.: +81 22 717 7284; fax: +81 22 717 7290.
E-mail address: kiinuma@ped.med.tohoku.ac.jp (K. Iinuma).

1059-1311/$30 – see front matter © 2004 Published by Elsevier Ltd on behalf of BEA Trading Ltd.
doi:10.1016/j.seizure.2004.04.003